ARE LARGE-APERTURE NbTi MAGNETS COMPATIBLE WITH 1E35?

E.Wildner, C.Hoa, E.Laface, G.Sterbini, CERN, Geneva, Switzerland

Abstract

To protect magnets in the insertion region, we have some degrees of freedom to use for optimal performance. Aperture, distance from the IP, the length of the magnets and the design of absorption systems are important parameters for the optimization. We look exclusively here at the effects of the collision debris, which give the major contribution to the heat deposition in the insertion magnets. To answer the challenging question in the title of this contribution, the approach was to use the baseline upgrade scenario for phase 1 and simply imagine higher particle fluxes from the higher luminosity (no change in optics). From this, a simple approach of magnet shielding using a liner in the cold bore tube gave us the answer: NbTi technology may be compatible with a luminosity of 10^{35}. This gives also the interesting possibility to extract heat from this liner at a higher cryogenic temperature. However the final demonstration needs a detailed model.

We have also made some parameter variations (crossing angle, TAS aperture) and checked the Q0 upgrade scenario concerning deposited heat. The effect of a D0 magnet on heat deposition in the IR has also been evaluated.

THE PHASE I UPGRADE SCENARIO

Two scenarios for the upgrade phase I have been studied, the first is the "symmetric, large aperture layout" [1] and one of the proposals in [2], the "compact, low gradient final focus system". The reason for taking this latter solution from [2] is to see the effect of the very large apertures. For the latter we have calculated two cases, the one proposed in the report and a second option where the length of the available LHC cable has been taken into account for the cross section design. The layout dimensions are shown in figures 1 and 2 and the magnets are described in table Table 1.

Figure 1: The Symmetric layout. The magnets have two cable layers. The cylinder to the left represents the TAS.

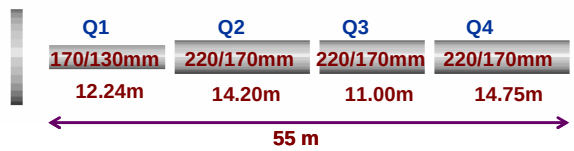

Figure 2: The Compact1 and Compact2 layouts. The Compact2 one has the largest aperture and only one cable layer.

Table 1: Magnet data

Magnet	MQCX	IRQB	IRQA	IRQF	IRQE
Layaout	Symm	Comp1	Comp1	Comp2	Comp2
Position	All	Q1	Q2-Q4	Q1	Q2-Q4
Gradient [T/m]	120	91.5	68.3	91.5	68.3
Aperture [mm]	130	170	220	130	170
Peak Field [T]	8.7	8.6	8.4	6.8	6.8
Layers	2	2	2	1	1

The quadrupole field maps have been calculated over 27 cm radius of the cold mass (value coming from the wanted grid of the field-map combined with the output data volume possibilities from field calculation software, for the time being) , which has been taken as the outer radius of the cold-mass. This means that we have to take into consideration that the total deposited heat in the structure may be larger for a larger volume of the cold mass. For comparisons and at this stage of the study this is good enough.

The collars have been modelled as aluminium with the idea to deposit energy far from the coils. For the energy in the coils this has minor impact and in future simulations we will replace aluminium with stainless steel in the collars for mechanical reasons.

The models contain cable insulation and cold bore insulation and this will be of importance in particular when the effects of irradiation will be simulated.

The parameters for the optics are, for all layouts, a betastar of 0.25 m and a vertical crossing angle of 220 micro radians. The collision points are simply modelled using Gaussian smearing of the collision points corresponding to the beam size and the bunch length.

6000 particles have been used for the Compact1 and Compact 2 models and 10000 for the Symmetric. This choice was only made from time constraints to finish the studies timely. For this preliminary study, analysis shows that the choice of a relatively small number of particles gives a good idea of the situation and refined studies will use sufficient number of particles to ensure less than 5 % statistical errors.

The TAS (Target Absorber for Secondaries) opening has been calculated using the formula

$$D_{\min} = 1.1 \cdot (9 + 2 \cdot 10)\sigma + 2(d + 3mm) + 2 \cdot 1.6mm$$

where the beam size is 1 σ, the beam separation 10 σ, d is the spurious dispersion orbit. The orbit excursion is 3 mm and mechanical tolerances have been taken as 1.6 mm. The factor 1.1 is the contingency for the beta-beating. For our case we used the value of 41 mm.

The opening of the TAS should be small to protect the magnet but sufficiently large not to intercept the beam. The efficiency of the TAS depends on the distance to the IP and of the free space available. Simulations of several insertion layouts show the TAS essentially protects the first 20 cm of the first quadrupole behind the TAS.

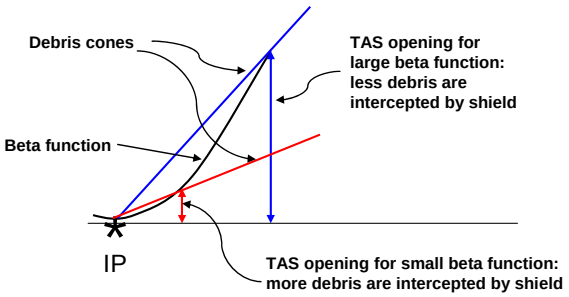

Figure 3: Illustration of important parameters for the TAS: For the case above: If he TAS is placed close to the IP where the beta-function is smaller (smaller beam size) then the opening of the TAS can be smaller.

RESULTS FROM THE CASE STUDIES

It is important to score the results from the simulations to correspond to the use of the information. We distinguish 3 different important quantities to be evaluated:

- Energy deposited in the cable (peak heat deposition)
  We make the binning for the scoring so that it corresponds to a maximum volume of equilibrium for the heat transport (cable transverse size, with a length of, in our case, 10 cm, which should correspond to the twist pitch of the cable). This is important to evaluate to see if there is a risk for quench.
- Total power deposited in the magnet
  It is important to know the volume of the magnet (the model has to be realistic) to be able to evaluate how much power has to be evacuated from the magnet structure.
- The power deposited per meter of magnet (a general overall estimate)

The results, calculated with FLUKA ([3],[4]), for the luminosity value of 2 10^{34} (corresponding to phase I) can be seen in Figure 4, the peak heat deposition along the magnets. First we can see that the 3 scenarios are similar, the largest aperture solution has the lowest heat deposition. We also see that there is an evident build-up in the first quadrupole. This build-up, including the part of the debris cone in between the two first quadrupoles seems to cause an important deposition peak on the front face of the second quadrupole. We can also see, that our present recommended limit of 4.3 mW/cm^3 (the quench limit/ 3) is exceeded.

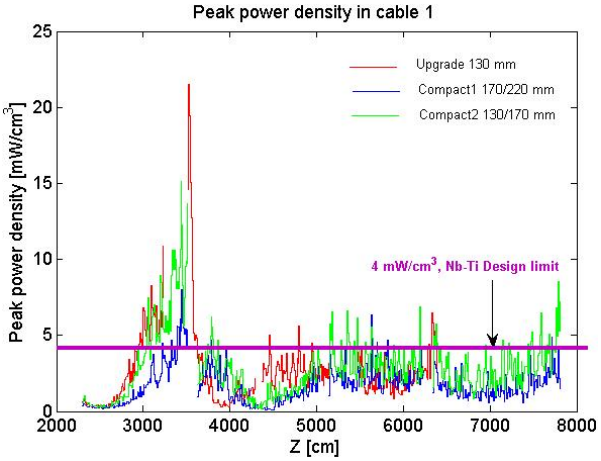

Figure 4: The peak heat deposition along the magnets in the inner triplet. The peak limit 4.3 mW/cm^3 is exceeded. The largest aperture solution is the best ("Compact 2").

In Figure 5 we see the total energy deposited in the triplet magnets. The "symmetric" solution has two times higher energy deposition than the other calculated upgrade scenarios, for magnets Q2a and Q3.

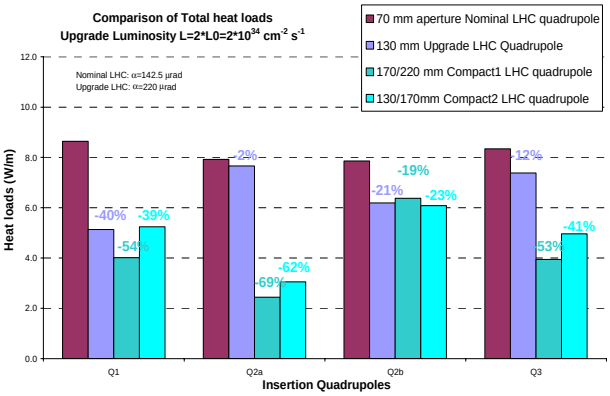

Figure 5: Total energy deposited in the triplet magnets. The 130 mm aperture solution ("Symmetric") has two times higher energy deposition than the other calculated upgrade scenarios for magnets Q2a and Q3.

Q0 OPTION

The Q0 option is described in [5]. The basic idea is to break the beta-function in a way that, in the triplet, we will have smaller beam-size which means smaller apertures. The layout is shown in Figure 6 and the magnet and optics parameters in Table 1 and in Table 2. The Q0 is close to the interaction point. This means less deposited

heat in the first magnets due to the fact that debris from the collision that contribute less to the deposited energy are intercepted at larger angles with respect to the magnet axes [6]. The energy deposition in the Q0 magnets and in the following triplet has been evaluated.

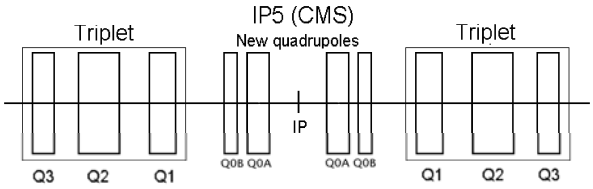

Figure 6: Q0 layout basic layout.

TABLE 1
MAGNET DATA FOR THE Q0 LAYOUT.

Magnet	L*[m]	Length [m]	Gradient [T/m]
Q0A	13.0	7.2	240
Q0B	20.8	3.6	196
Q1	25.8	8.6	200
Q2	37.1	11.5	172
Q3	52.0	6.0	160

TABLE 2
MAXIMUM BETA FUNCTION AND APERTURE IN MAGNETS FOR THE Q0 LAYOUT.

Magnet	β_{max}[m]	D_{min} [mm]
Q0A	2300	57.0
Q0B	4300	68.5
Q1	5780	75.2
Q2	5820	75.4
Q3	5770	75.1

The result for the deposited peak power distribution is shown in Figure 7. The peaks are more pronounced than for the Symmetric and the Compact cases. The apertures are smaller and this may be the reason for the higher deposition in spite the fact that the magnets are positioned close to the IP, which normally gives a reduction in the deposition [6]. This case has to be run with larger apertures to be comparable. The present Q0 layout gives peaks largely above the recommended limits. The overall deposited power is shown in Figure 8. Except at some local positions, the deposited power is below 10 W/m.

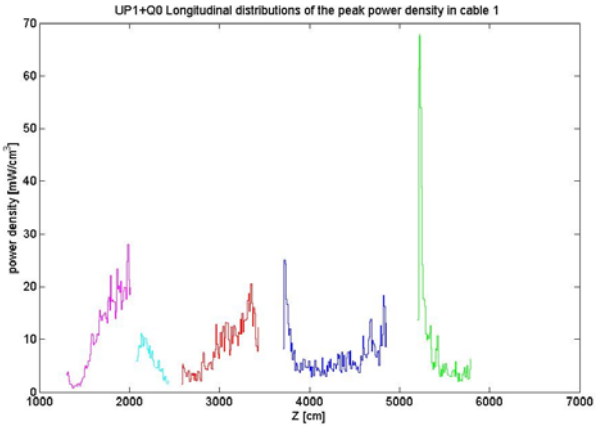

Figure 7: The longitudinal distribution of the peaks in the Q0 option scenario. The peaks are higher than for the Symmetric and Compact cases. The recommended limit is 4.3 mW/cm^3.

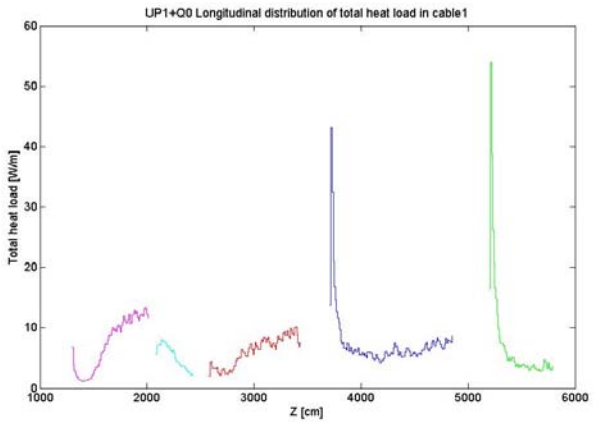

Figure 8: The total heat load along the Q0 doublet and the triplet, integrated over the azimuth.

In Figure 9 we see a 3D plot of the innermost cable of the first magnet Q0A, a smooth build-up along the magnet where the influence of the magnetic field can be distinguished

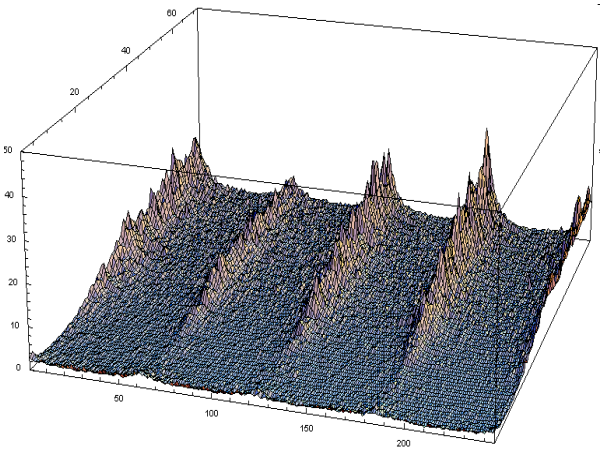

Figure 9: Energy deposition in the inner cable of Q0A

. The same plot for the second magnet in the triplet (Figure 10) shows a smoothed out energy deposition.

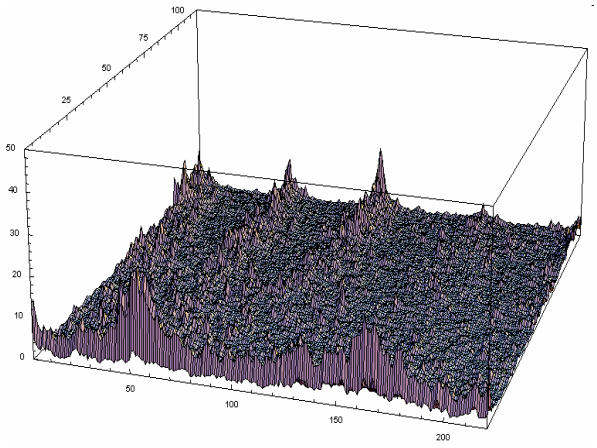

Figure 10: Energy deposition in the inner cable of the second triplet magnet.

Approximate values for the total power deposited in the Q0 magnets, assuming a design like described in [7] we get for Q0A a value of 106 W (14.7 W/m) and for Q0B a value of 42.5 W (11 W/m). The triplet magnet design has to be improved to give a reasonable indication of the total power. However, the power deposited in the triplet magnet cables gives a good first indication of the peak power deposited.

The apertures of these magnets are not comparable to the magnets used in the other scenarios. The present layout has high energy deposition that can possibly be reduced by opening the apertures as in the other cases. This remains to be checked.

PROTECTING THE IR MAGNETS

As described in [8] the deposited energy can be absorbed by a sufficiently thick liner. Figure 11 shows the effect of a thick liner: the peaks are absorbed in the liner and the coil is protected. The thickness of the liner has been estimated simply from the extension of the high energy deposition region in Figure 11 adding some small margin for the closeness to the beam axis where particle energies are higher. The aperture has, in a final design, to be large enough for the beam requirements (optimization).

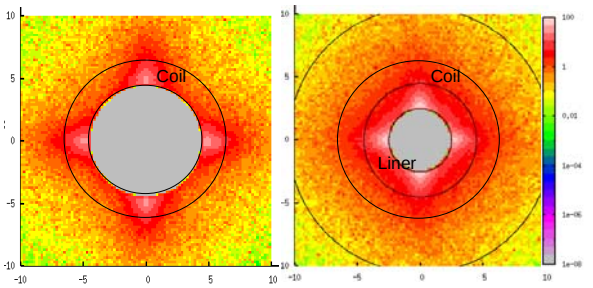

Figure 11: Absorbing the peaks of the energy deposited in the quadrupoles: To the left without liner and to the right a thick liner is inserted inside the aperture to protect the coil from the deposition peaks.

In addition we have checked the effect of a mask. See Figure 12. The idea of this mask is to collect the particles accumulating between the magnets and impinging on the surface of the downstream magnet.

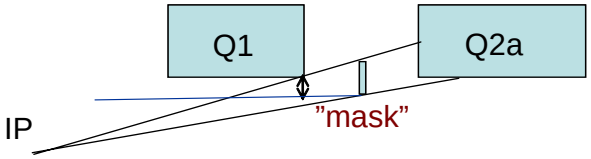

Figure 12: The idea of the mask is to absorb the energy built up between the magnets.

The configuration that was implemented is shown in Figure 13. One case with a small tungsten mask of 1 cm thickness, 10 cm long and one case with a liner of 2 cm stainless steel have been tested. The implementation has to be optimized.

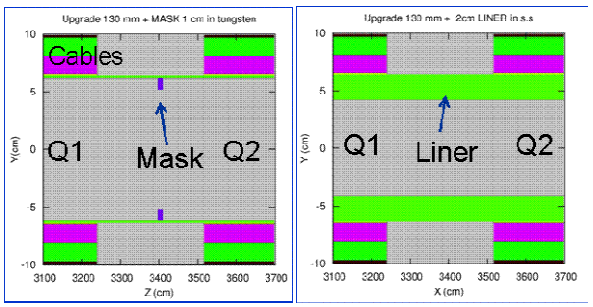

Figure 13: Left, a small mask inserted inside the beampipe, right a thick liner inside the beampipe.

The result of the calculations is displayed in Figure 14. The peaks are considerably reduced. For the thick liner the reduction is 95% and for the small mask inserted in

from of the second quadrupole the reduction is 36%. This is a good indication that with correctly dimensioned apertures and liners we should be able to protect the coils from the collision debris.

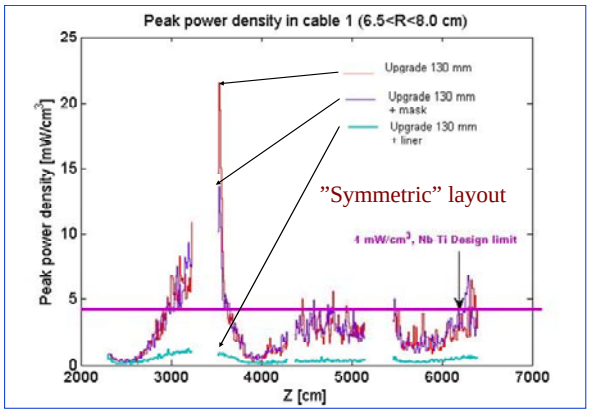

Figure 14: Implementing absorbers reduces the pek power deposition. The mask reduces the peak in the second quadrupole by 36% and the thick liner reduces the peaks by 95% in this case.

The total energy deposition in the magnets decrease around 30% if a liner is introduced. A small mask is inefficient for the total heat load.

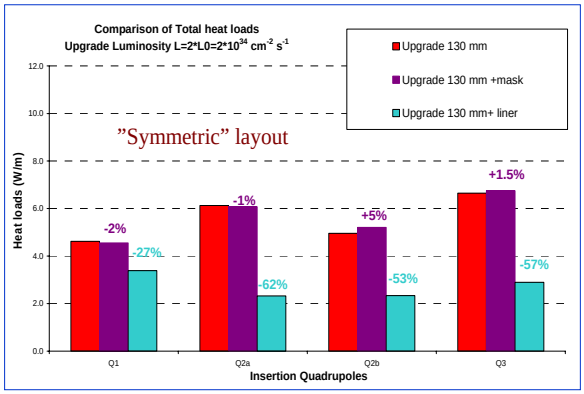

Figure 15: The total heat load for the "symmetric" layout, original layout and layout with mask and with liner.

EXTRAPOLATION TO PHASE II

From the results discussed in the previous paragraph we can answer the question in the title: there is no indication that we cannot with some optimization (future work) of the magnets and using realistic liner thicknesses and material to have sufficient apertures it seems possible to stay below the limits for the deposited peak energy deposition in the NbTi coils (4.3 mW/cm^3). We have to scale the results above to 5 times higher energy deposition values, since the upgrade phase II luminosity is 5 times higher and energy deposition scales linearly. We have assumed, for this exploratory study, that the layout and optics are similar for phase one and for phase. However, the optics is not yet defined: betastar may be lower than in our study and magnet apertures and lengths may change. This may also alter the collision conditions and needs a refined study on the proton distributions in the collision points. The crossing angle impact has to be checked and taken into account, the crossing angle changes for different Luminosity options. Some magnetic arrangements may also help; for example the D0 option has been checked to see if a chicane has an effect on the collision debris impact on the triplet magnets.

CROSSING ANGLE

The effect of the crossing angle for the "symmetric" proposal of the triplet upgrade has been investigated and is displayed in Figure 16. There is a 20% increase in the peak at the entrance of Q2a and some additional peak build-up in Q1 and Q3 if the crossing angle is increased from 142.5 µrad to 220.0 µrad. The crossing angle is vertical in our calculations and analysis has to be done also for the effect of the horizontal crossing angle and the effect of the D0 deflecting in the same plane as the crossing scheme.

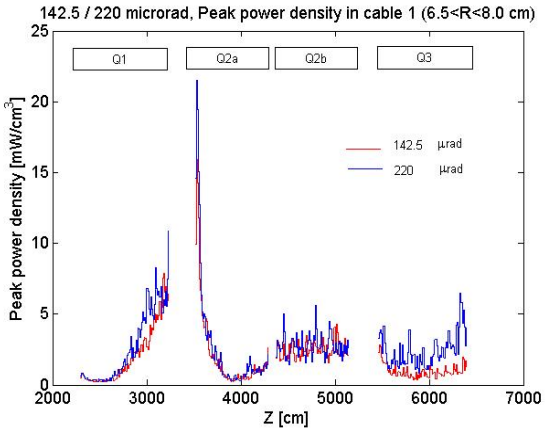

Figure 16: Peak energy deposition for 142.5 µrad and 200.0 µrad vertical crossing angle.

The total deposited energy is changed only marginally, see Table 3, "Symmetric" upgrade case, vertical crossing angles. For For Q2b the energy deposition decreases for the others there is a small increase. The total in the quadrupoles increases by 7 % when the crossing angle increases from 142.5 µrad to 220.0 µrad.

TABLE 3
POWER DEPOSITED [W] IN THE INSERTION ELEMENTS FOR TWO DIFFERENT CROSSING ANGLES IN THER VERTICAL PLANE.

Element	142.5 [µrad]	220.0 [µrad]
TAS	321.2	315.6
BP	15.4	16.8
Q1	46.5	48.2
Q2a	54.9	59.7
Q2b	50.0	48.3
Q3	60.4	69.4
Total Quads	211.9	225.7

TAS OPENING

The effect of the TAS has been evaluated. We can see in Figure 17 the effect of the TAS, the effect is only detectable for the first quadrupole, the Q1. The TAS absorbs essentially particles impinging head on the magnet entrance. The magnets downstream of the TAS absorb essentially particles coming from inside the beam-pipe.

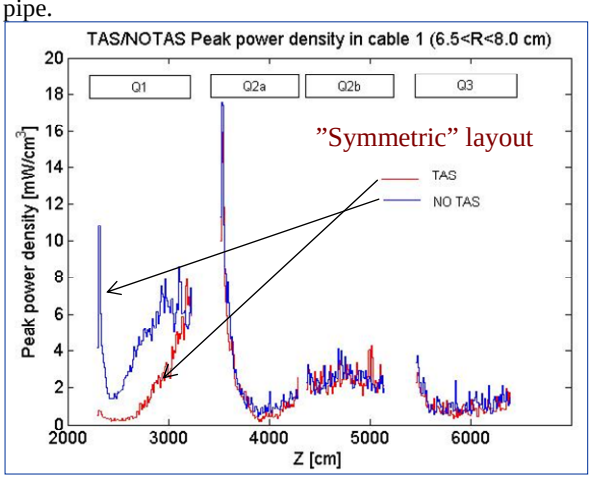

Figure 17: The effect of the TAS can be observed only for the first quadrupole.

Different apertures of the TAS, from 36 mm to 42 mm in steps of 2 mm, have also been calculated. As expected a larger TAS opening affects the Q1 quadrupole; a larger aperture TAS means a somewhat higher energy deposition on the fist magnet (approximately 10% per every 2 mm). However for the other triplet magnets the effect is marginal, see Figure 18.

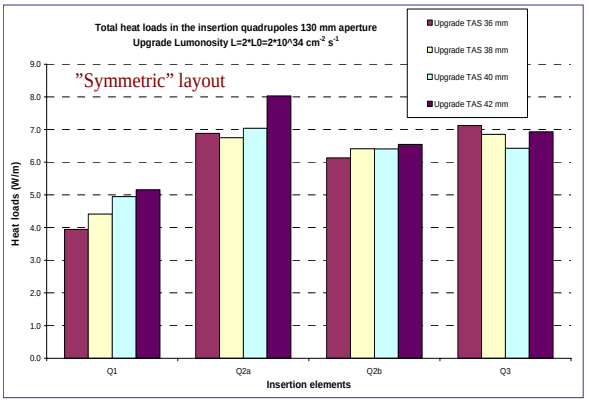

Figure 18: The TAS aperture has been varied and on the first quadrupole the effect is larger with increasing TAS aperture. For the following quadrupoles the effect is less evident.

EFFECTS OF THE D0 SCHEME

The fact that the debris products have different magnetic rigidities than the beam may be used in a chicane to filter the unwanted particles. The effect of D0, see [8] for this proposal, can be good in this respect to protect the magnets. In Figure 19 we see the D0 magnet, placed only 3m from the IP. The field is 3 T and the length of the magnet is 2 m.

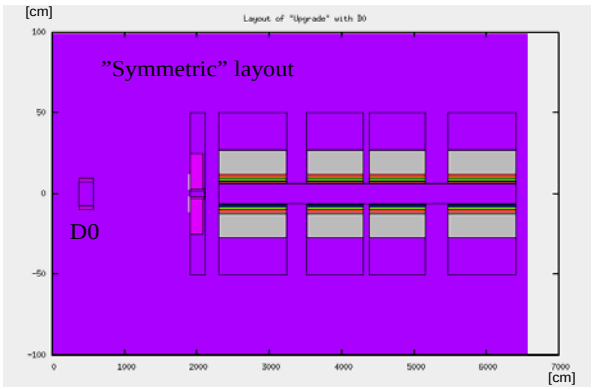

Figure 19: The D0 magnet is placed 3m from the IP, its field is 3T, the length is 2 m and the aperture is 15cm. D0 is deflecting horizontally in this example.

The total deposited energy is spread over the TAS and is less penetrating into the triplet. See Figure 20 where the TAS can be seen inside the aperture of the magnet and absorbing more energy when the D0 field is present (right) than in the case with no D0 effect (left).

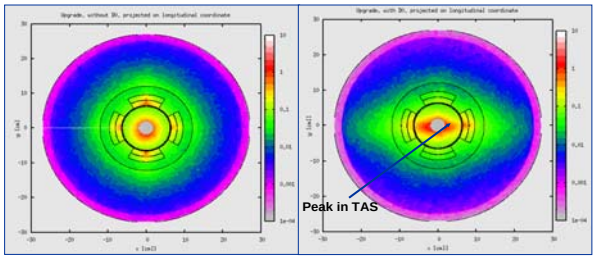

Figure 20: Effect of the vertical field D0 (transverse projection).

The peaks are changed azimuthally between a case with vertical crossing and a horizontal field of the D0 (This combination is just for demonstration of the effect), see Figure 21We see an impact of the D0 also on the peak energy deposited in the inner cable of the quadrupoles, see effect in Q2a in Figure 21.

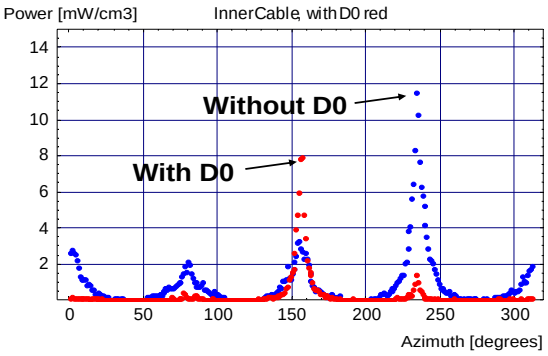

Figure 21: D0 redistributes the energy deposition, here is shown the azimuthal distribution of the peak energy deposited in the inner cable for the longitudinal scoring bin (slice) with the highest peak.

CONCLUSION

We have indications that the energy deposited in the triplet magnets for the upgrade scenarios chosen in this study (the "symmetric" 130 mm aperture and the very large aperture "compact" layouts) could be handled by optimized absorbing systems even for luminosities up to 10^{35}. However, the study is made using a scaling of the Phase I solution and further studies have to be made for a real phase II case.

The aperture of the TAS is influencing essentially the first quadrupole in the triplet. The D0 scheme has an important impact on the energy deposition and has to be carefully studied for all crossing angles; the crossing angle has also an impact on the deposited energy.

REFERENCES

[1] J. P. Koutchouk, L. Rossi, E. Todesco, "A Solution for Phase-one Upgrade of the LHC Low-beta Quadrupoles Based on Nb-Ti", LHC Project Report 1000.

[2] O. Brüning, R. De Maria, R. Ostojic, "Low Gradient, Large Aperture IR Upgrade Options for the LHC compatible with Nb-Ti Magnet Technology", LHC Project Report 1008.

[3] 'FLUKA: a multi-particle transport code', A. Fasso`, A. Ferrari, J. Ranft, and P.R. Sala, CERN-2005-10 (2005), INFN/TC_05/11, SLAC-R-773

[4] 'The physics models of FLUKA: status and recent developments', A. Fasso`, A. Ferrari, S. Roesler, P.R. Sala, G. Battistoni, F. Cerutti, E. Gadioli, M.V. Garzelli, F. Ballarini, A. Ottolenghi, A. Empl and J. Ranft, Computing in High Energy and Nuclear Physics 2003 Conference (CHEP2003), La Jolla, CA, USA, March 24-28, 2003, (paper MOMT005), eConf C0303241 (2003), arXiv:hep-ph/0306267.

[5] E. Laface et al., "Interaction Region with Slim Quadrupoles", CERN-LHC-Project-Report-970, Geneva 2006

[6] Christine Hoa: "Procedures and first investigation of the power radiated by proton-proton collisions into an early separation dipole for the LHC Luminosity Upgrade",LHC Project Note 395.

[7] Elena Wildner: "Heat deposition and backscattering for one of the configurations of the IR for LHC upgrade", Internal Note CERN/AT/MCS/ Mars 2007

[8] J.-P. Koutchouk, G. Sterbini, "An Early Beam Separation Scheme for the LHC Luminosity Upgrade", CERN-LHC-Project-Report-972, Geneva, 2006